Applied Catalysis B: Environmental 113–114 (2012) 160–171

Contents lists available at SciVerse ScienceDirect

Applied Catalysis B: Environmental

journal homepage: www.elsevier.com/locate/apcatb

Mono- and bimetallic Rh and Pt NSR-catalysts prepared by controlled deposition of noble metals on support or storage component

Robert Büchel[a,b], Sotiris E. Pratsinis[a], Alfons Baiker[b,*]

[a] Particle Technology Laboratory, Department of Mechanical and Process Engineering, ETH Zurich, Sonneggstrasse 3, CH-8092 Zurich, Switzerland
[b] Department of Chemistry and Applied Biosciences, ETH Zurich, Hönggerberg, HCI, CH-8093 Zurich, Switzerland

ARTICLE INFO

Article history:
Received 5 September 2011
Received in revised form
16 November 2011
Accepted 18 November 2011
Available online 28 November 2011

Keywords:
Flame spray pyrolysis
NO_x storage-reduction (NSR)
Mono- and bimetallic catalyst
Platinum
Rhodium
Alumina
Barium carbonate
Selective deposition
Fast NO_x storage
Lean NO_x trap
Sulfur poisoning

ABSTRACT

Mono- and bimetallic Rh and Pt based NO_x storage-reduction (NSR) catalysts, where the noble metals were deposited on the Al_2O_3 support or $BaCO_3$ storage component, have been prepared using a twin flame spray pyrolysis setup. The catalysts were characterized by nitrogen adsorption, CO chemisorption combined with diffuse reflectance infrared Fourier transform spectroscopy, X-ray diffraction, and scanning transmission electron microscopy combined with energy dispersive X-ray spectroscopy. The NSR performance of the catalysts was investigated by fuel lean/rich cycling in the absence and presence of SO_2 (25 ppm) as well as after H_2 desulfation at 750 °C. The performance increased when Rh was located on $BaCO_3$ enabling good catalyst regeneration during the fuel rich phase. Best performance was observed for bimetallic catalysts where the noble metals were separated, with Pt on Al_2O_3 and Rh on $BaCO_3$. The Rh-containing catalysts generally showed much higher tolerance to SO_2 during fuel rich conditions and lost only little activity during thermal aging at 750 °C.

1. Introduction

Traditional three-way catalysts [1] cannot efficiently reduce NO_x to N_2 under oxygen rich conditions that are encountered in fuel lean combustion and direct injection engines. Therefore, selective catalytic reduction (SCR) [2] and NO_x storage-reduction (NSR) catalysts have been developed [3]. In the latter process, the exhaust NO_x is trapped under oxygen rich conditions on an alkali or alkaline-earth metal (e.g. K, Ba) mainly in the form of corresponding metal nitrates [4]. Because NSR catalysts do not need an additional reducing fuel (like NH_3 or urea as in SCR) and require less mounting space, they are particularly attractive for compact cars [5]. Drawbacks of NSR catalysts are connected with deterioration [6], thermal aging [7] and sulfur poisoning [8]. Sulfur typically present in the fuel and lubricant oils [9] is oxidized to SO_2 during combustion. The SO_2 in the exhaust gas can adsorb on the catalyst and poison it. As-poisoned catalysts typically require regeneration temperatures above 700 °C [10]. Catalyst deactivation was found to be strongest by SO_2, compared to other sulfur-containing species like H_2S and COS [11]. Furthermore, SO_2 deactivates NSR catalysts faster during the fuel rich periods [12].

The effect of SO_2 on the storage component and the noble metal are different [12]: As concerns the noble metal, SO_2 can have negative as well as positive influence on the catalyst's oxidation activity e.g. while 20 ppm SO_2 decreased the activity for propene oxidation of Pt/Al_2O_3 catalysts, the same concentration of SO_2 had a positive effect on propane oxidation [13] because PtO_2 is reduced in the presence of SO_2 to Pt [14]. In contrast to Pt, for Rh no loss of NO reduction activity was observed in the presence of SO_2 [15]. Furthermore Rh is a highly active NO reduction catalyst [16] that enhances the regeneration of Ba-nitrates [17]. After regeneration of H_2S poisoned catalysts, Rh showed the highest CH_4 oxidation performance among alumina supported Pt, Pd or Rh catalysts [18]. In the presence of SO_2, the NO_x reduction activity of Pt based catalysts decreases while that of Rh catalysts is less affected [19]. For Rh, however, the NO_x oxidation is inhibited in the presence of SO_2, while Pt shows considerable tolerance [20]. Combinations of Pt and Rh maintained their activity for the entire NSR process [21]. Also for CO/hydrocarbon mixtures, combinations of Pt and Rh gave better performance than either metal alone [22]. Computational analysis

* Corresponding author. Tel.: +41 44 632 31 53; fax: +41 44 632 11 63.
E-mail address: alfons.baiker@chem.ethz.ch (A. Baiker).

0926-3373/$ – see front matter © 2011 Elsevier B.V. All rights reserved.
doi:10.1016/j.apcatb.2011.11.033

predicted the segregation of Rh to the surface of Pt for combined Rh/Pt systems [23].

Sulfur compounds can also chemisorb on the storage component finally forming sulfates [24], e.g. $BaSO_4$ which decomposes at higher temperatures than $Ba(NO_3)_2$ and thus lowers the number of Ba-sites active in NO_x storage. The rate of NO_x uptake was found to decrease proportionally to the SO_2 dosing, indicating that the amount of SO_2 uptake is more important than the actual SO_2 concentration for catalyst deactivation [25].

With flame spray pyrolysis (FSP) a variety of materials for different catalytic applications have been synthesized [26]. For NSR catalysts, a two-nozzle FSP setup was used to produce the Ba and Al components separately [27]. The as-formed $BaCO_3$ is finely dispersed on the support and can decompose to BaO and CO_2 below 600 °C [28]. Additionally, the two-nozzle FSP allows preferential deposition of noble metals on the storage or support components [29]. Also bimetallic Pt/Pd clusters were produced with FSP [30]. These bimetallic systems were more stable at higher temperature (1000 °C) [31] than corresponding monometallic ones, and had higher sulfur tolerance [32] and oxidation activity [33]. It was shown previously that the location of the noble metal is important in NSR: While Pt on Al_2O_3 showed a high NO oxidation activity [34], Pt on the Ba component showed a tendency to form PtO_x which is less active than Pt^0 for NO oxidation [35]. Nevertheless, Pt on the Ba component also promotes $Ba(NO_3)_2$ decomposition leading to good regeneration of the Ba storage component and long cycle life [36].

Here, we investigated the structural and catalytic properties of mono- and bimetallic Rh and Pt based NSR catalysts where the noble metals were preferentially deposited either on the alumina support or on the storage component ($BaCO_3$). The influence of the noble metals and their location on the NSR performance was investigated in the absence and presence of SO_2 in the feed gas.

2. Experimental

Mono- and bimetallic alumina-supported Rh and Pt catalysts containing $BaCO_3$ as storage component were prepared using a two-nozzle FSP [27] unit with a two-nozzle angle of 160° to ensure the preferential deposition of noble metals [29]. Each nozzle used a premixed CH_4/O_2 flame at a volume ratio of 1/2 to ignite and sustain the spray [37]. The Al-precursor solution consisted of aluminum-tri-*sec*-butoxide (Fluka, 95%) dissolved in a 2:1 vol. ratio of diethylene glycol monobutyl ether (Fluka, 98%) and acetic anhydride (Riedel-de Haën, 99%). The aluminum concentration was kept constant at 0.5 mol/L. The Ba-precursor solution consisted of barium 2-ethylhexanoate (Aldrich, 98%) dissolved in 1:1 vol ratio of toluene (Riedel-de Haën, 99%) and 2-ethylhexanoic acid (Riedel-de Haën, 95%) for a Ba concentration of 0.06 mol/L. Appropriate amounts of Rh(III)-acetylacetonate (Sigma–Aldrich, 99.99%) and/or platinum(II) acetylacetonate (Alfa Aesar, 98%) were added either to the Ba- or Al-solutions. The Ba- and Al-precursor solutions were sprayed at 3 and 5 ml/min, respectively, and both were dispersed with 5 L/min O_2 (Pangas, 99,95%) each. The Al-, Ba-, Rh/Pt-concentration and spray rates were chosen to result in a nominal (Rh + Pt)/Ba/Al_2O_3 weight ratio of 1/20/100. This corresponds to a noble metal weight loading of 0.78 wt%, assuming that all Ba is present as $BaCO_3$ [28]. Note that the flame made catalysts were not subject to an additional temperature pretreatment as usually applied for conventionally prepared catalysts.

In the notation used here, the noble metal and its mass relative to the support are written next to the material with which it was co-produced, and therefore preferential deposition on these components is expected [36]. For example, 0.5PtAl-Ba0.5Rh means that Pt-acetylacetonate was dissolved in the Al-precursor solution and Rh-acetylacetonate was dissolved in the Ba-precursor solution with a weight ratio of Rh/Pt/Ba/Al_2O_3 of 0.5/0.5/20/100. With bimetallic catalysts we distinguish between "separated" and "mixed" catalysts. In the former the two metals were deposited on different constituents (support, storage), in the latter the two metals were deposited without preferential deposition. For comparison a Pt/Ba/Al_2O_3 reference catalyst was prepared by means of wet-impregnation according to the procedure reported in [38].

Nitrogen adsorption–desorption isotherms were measured at 77 K using a Micromeritics Tristar instrument. The BET method was used to determine the specific surface area (SSA) by a 5-point nitrogen adsorption isotherm. The estimated accuracy is ±3%. X-ray diffraction (XRD) patterns were recorded with a Bruker D8 Advance instrument (40 kV, 40 mA, $\lambda = 0.154$ nm). Crystallite sizes and mass fractions were calculated using the fundamental parameter approach and the Rietveld method with the TOPAS 3 software at ±10% accuracy [36].

For scanning transmission electron microscopy (STEM), the catalyst material was dispersed in ethanol and deposited onto a perforated carbon foil supported on a copper grid (Okenshoji Co. Ltd.). The STEM images were obtained with a high-angle annular dark-field (HAADF) detector attached to a Tecnai 30F microscope (FEI; field emission cathode, operated at 300 kV), showing the metal particles with bright contrast (Z contrast). For qualitative analysis, the electron beam was set to selected areas in the STEM images and the signal was measured by energy dispersive X-ray spectroscopy (EDXS; detector: EDAX).

The amount of CO chemisorbed on the noble metals was measured using a Micromeritics Autochem II 2920 with 10 CO-pulses at 40 °C after pretreating the catalysts at 300 °C under 5% H_2/Ar [28]. Diffuse reflectance infrared Fourier transform spectroscopy (DRIFTS) was carried out with a VECTOR 22 spectrometer (Bruker Optics). Spectra were obtained by averaging 100 scans at 4 cm^{-1} resolution. The average stoichiometric factor (SF) of chemisorbed CO was determined by taking the ratio from the peak area between linear and bridged bonded CO [39] of the spectrum at ±5% accuracy. Band positions below 1950 cm^{-1} were considered as bridged bound CO, while linear bound CO is that between 2100 cm^{-1} and 1950 cm^{-1} [40]. A sensitivity ratio of 0.8 for bridged CO with respect to linear bond CO was assumed based on previous DFT simulations [41]. The average noble metal dispersion (%) was calculated from the specific CO uptake mol_{CO}/mol_{metal} multiplied with the corresponding average stoichiometric factor (SF) determined by DRIFTS.

For NSR testing, the as prepared powder was pelletized (5.9 kg/mm^2), ground and sieved: 20 mg of catalyst with 0.08–0.14 mm size fraction were mixed with inert 383 mg SiC (size fraction 0.18–0.24 mm) and was placed in a quartz glass reactor with an inner diameter of 4 mm, resulting in a catalyst bed length of 2 cm. The time to equilibrate between lean and rich mixtures (measured with inert SiC materials) was approximately 90 s. The as-prepared catalyst was heated up to 300 °C under 300 ml/min He. A schematic of the reactor setup and the experimental procedure applied for the catalytic tests is shown in Fig. 1. With mass flow controllers (Brooks, 5850S) the O_2 (Pangas, 99.95%), C_3H_6 (Pangas, 1% in He), NO (Linde, 1% in He) and He (Pangas, 99.996%) were mixed to a total of 500 mL/min (assuming a void space of 0.4 this results in a space velocity of 300,000 h^{-1}) of fuel lean (400 ppm NO, 500 ppm C_3H_6, and 8% O_2, balance He), and fuel rich gases (400 ppm NO and 500 ppm C_3H_6, balance He), similar to Amberntsson et al. [21]. Note that this space velocity is considerably higher than the space velocities often used in model type studies which range between 10,000 and 120,000 h^{-1} [42,43]. We have used this high space velocity because it allowed a better discrimination between the performances of the different catalysts. Furthermore it is interesting to explore the catalytic performances at higher space velocity because these experiments give a rough idea where the limitations

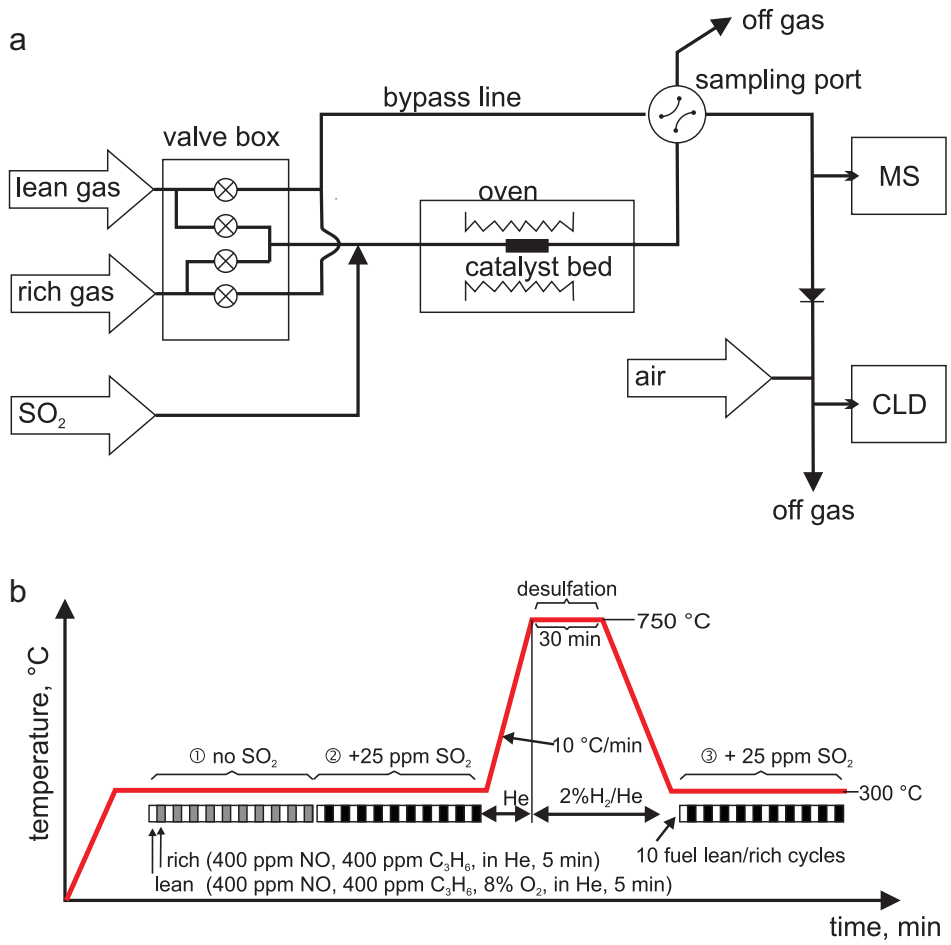

Fig. 1. Scheme of experimental setup (a) and procedure applied in catalytic tests (b).

with regard to the compacting of catalytic converters are. For comparison some experiments were also carried out at a lower space velocity of 38,000 h^{-1}. With six control valves, the feed was controlled in a way that either fuel lean or rich gas flowed through the catalyst bed, while the other gases were flowing through the by-pass line to the sampling port.

The horizontally oriented oven (HTM Reetz, LK1100-40-400-2) allowed to heat the catalyst up to 1100 °C. All gas lines (stainless steel) were heated to 120 °C to prevent water condensation. At the sampling port either the catalyst off-gas or the gas from the bypass line was selected to calibrate the inlet concentration. The off-gas was analyzed with a quadrupol mass spectrometer (MS; Pfeiffer vacuum, ThermoStar GSD 301) and a chemiluminescence detector (CLD; ECO Physics, CLD 822S). Before the CLD, the off-gas was diluted with 400 mL/min air. Previously fast FTIR analysis for experiments with similar materials showed no formation of NH_3, and N_2O only for short periods of about 20 s when switching from fuel rich to fuel lean conditions [44].

The catalyst test procedure is illustrated in Fig. 1b. Catalytic performance was tested first for 10 cycles without sulfur dioxide, then for 10 cycles with 25 ppm SO_2 (2.5 mL/min, 5000 ppm SO_2 in N_2, Pangas) while each cycle exposed the catalysts 5 min to a fuel lean and 5 min to a fuel rich gas composition. Note that these cycling periods were chosen due to some constrains given by the experimental setup used. The catalyst was then heated to 750 °C at 10 °C/min under 500 mL/min He and then held isothermally at this temperature for 30 min. There, the catalyst was reduced with 2% H_2 in He (500 mL/min) and cooled down to 300 °C where the catalyst was tested again for 10 fuel lean/rich cycles in the presence of 25 ppm SO_2. For each cycle the integral NO_x conversion for each cycle was calculated as: $NO_{x,conv} = (NO_{in} - NO_{x,out})/NO_{in}$. When repeating measurement with fresh material the reported values varied by less than 10%. The stored NO_x was calculated by integration of the NO_x stored on the catalyst during the fuel lean phase. The reported values are representative values, after the storage and reduction cycles reached steady-state: the durations of the different measurement series 1–3 were: 1) 40–50 min (without SO_2), 2) 160–170 min (with 25 ppm SO_2), and 3) 472–482 min (with SO_2, after desulfation). The estimated accuracy was ±5%. In order to account for possible NO_x uptake and conversion caused by the experimental setup, blind tests with inert material (SiC) were performed. These blind tests indicated NO_x consumption of <4% which has been taken into account in the data evaluation. Complete saturation experiments were performed under the same gas flow conditions but the cycle length was extended to 2 h (1 h lean and 1 h rich) and the cycles were repeated 4 times without SO_2 followed by 3 cycles in the presence of 25 ppm SO_2. All gas flows were calibrated to 0 °C (Bios, Definer 220) with an accuracy of ±1%.

3. Results and discussion

3.1. Structural properties of catalysts

Four types of $M/BaCO_3/Al_2O_3$ NSR catalysts with different noble metal (M) composition were synthesized using the twin nozzle system: Monometallic Rh and Pt catalysts as well as bimetallic *mixed*

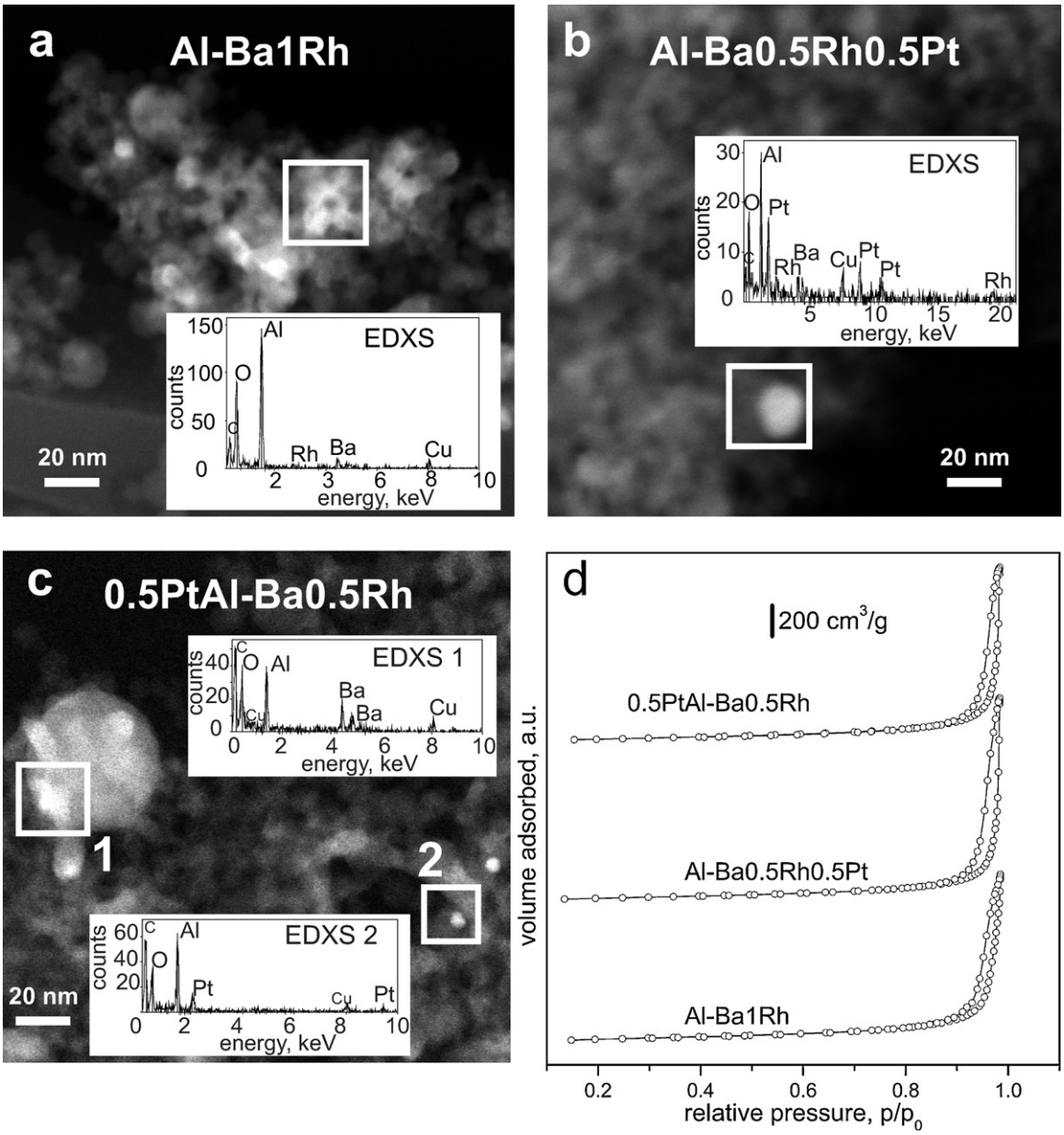

Fig. 2. STEM and EDXS of indicated area for selected catalysts (a). Al-Ba1Rh, (b) Al-Ba0.5Rh0.5Pt, and (c) 0.5PtAl-Ba0.5Rh. The Cu signal in the EDXS is due the support grid. In (d) BET isotherms of these particles are shown, indicating that they are non-porous.

Rh/Pt, and *separated* Rh and Pt catalysts. In *mixed* Rh/Pt catalysts both noble metal precursors were fed through the same nozzle resulting in their deposition on both the support (γ-Al_2O_3) and storage component ($BaCO_3$). In *separated* Rh and Pt catalysts one noble metal was deposited on the support and the other on the storage material. We have demonstrated in a previous study by means of electron microscopy combined with EDX [36] that the twin nozzle system applied for the synthesis of the catalysts effectively allows the preferential deposition of noble metal particles on either the storage or support material. Here we used DRIFTS measurement with CO to estimate approximate mean stoichiometric factors of the CO adsorption and to gain some information about the oxidation state of the noble metals.

Fig. 2a–c shows for selected catalysts the typical STEM images with EDXS of the highlighted area. The Rh signal in EDXS was difficult to detect as seen for Al-Ba1Rh (Fig. 2a) probably due to the lower X-ray yield of Rh (Z = 45) compared to Ba (Z = 56) and Pt (Z = 78). Only in bimetallic *mixed* Al-Ba0.5Pt0.5Rh (Fig. 2b) simultaneously Rh and Pt were detected. In the bimetallic *separated* 0.5PtAl-Ba0.5Rh (Fig. 2c) the Ba and Pt were not detected together as expected for preferential deposition. The Cu and part of the C signal are due to the Cu containing grid. All the flame-derived catalyst powders were virtually nonporous as indicated by the typical nitrogen adsorption-desorption isotherms observed (Fig. 2d), which all showed a hysteresis at high relative pressure due to the interparticle void space of the powders.

Some properties (BET surface areas, $BaCO_3$ and Al_2O_3 crystallite sizes, CO adsorption uptake, stoichiometric factors of CO adsorption and average metal dispersion) of the flame derived catalysts are listed in Table 1. The surface area (SSA) for Rh-containing catalysts was fairly constant (161–170 m^2/g). The Pt-only catalysts showed a slightly lower SSA (124–137 m^2/g). This may be attributed to the fact that the total noble metal weight was fixed to 0.78 wt% resulting in almost two times higher number of Rh than Pt atoms due to the much lower atomic weight of the former (A_{Rh} = 102.9 g/mol, compared to Pt (A_{Pt} = 195.1 g/mol). Interestingly, a similar

Table 1
Structural properties of flame-made catalysts. Specific surface area (SSA), specific CO uptake, average stoichiometric factor (SF), and noble metal dispersion.

	Catalyst	SSA[a] (m^2/g)	d_{BaCO_3}[b] (nm)	$d_{Al_2O_3}$[c] (nm)	CO adsorption ($mol_{CO}/mol_{(Rh+Pt)}$)	SF[d]	Dispersion (%)
Monometallic							
Rh-only	1RhAl–Ba	161	8	9	0.23	1.01	23
	Al–Ba1Rh	163	5	12	0.06	1.17	6
Pt-only	1PtAl–Ba	124	8	10	0.24	1.16	24
	Al–Ba1Pt	137	7	12	0.22	1.30	22
Bimetallic							
Mixed Rh/Pt	0.5Rh0.5PtAl–Ba	170	8	10	0.24	1.04	24
	Al–Ba0.5Rh0.5Pt	163	6	9	0.10	1.13	10
Separated Rh and Pt	0.5RhAl–Ba0.5Pt	170	8	8	0.36	1.25	36
	0.5PtAl–Ba0.5Rh	167	7	9	0.15	1.22	15

[a] Specific surface area (SSA) measured with BET method.
[b] Mean crystallite size of as prepared $BaCO_3$ by X-ray line broadening of (1 1 1) monoclinic $BaCO_3$.
[c] Mean crystallite size of Al_2O_3 determined by X-ray line broadening of (2 2 4) reflections.
[d] Stochiometric factor (SF) determined from DRIFT measurements and used to calculate the noble metal dispersion.

contribution to the surface area was not observed with correspondingly prepared Pd (A_{Pd} = 106.4 g/mol) catalysts [30] which showed about the same SSA (130 m^2/g) as the Pt catalysts. Corresponding flame-made pure γ-Al_2O_3 and $BaCO_3$ showed SSAs of 148 m^2/g and 20 m^2/g, respectively [36].

The bulk structure of as-prepared catalysts was determined by powder XRD (Fig. 3). Fresh as-prepared powders showed the monoclinic $BaCO_3$ phase that transforms after some days, into the more stable orthorhombic $BaCO_3$ [45]. The reported crystallite sizes of $BaCO_3$ refer to as-prepared powders, where no orthorhombic $BaCO_3$ was observed. Mean crystallite sizes derived from X-ray line broadening for the storage and support components were (Table 1): $BaCO_3$, 5–8 nm; Al_2O_3, 8–12 nm.

CO adsorption measurements clearly showed higher CO uptake for catalysts where Rh was deposited on alumina, while Rh deposition on $BaCO_3$ resulted in low CO uptake indicating low dispersion. This is attributed to both the higher specific surface area of Al_2O_3 compared to $BaCO_3$ as well as the difference in surface properties between these materials e.g. the acid–base properties and wetting angle [46]. The noble metal dispersion ranged from 6% (Al-Ba1Rh) to 36% (0.5RhAl-Ba0.5Pt).

DRIFTS measurements of CO adsorption (Fig. 4) provided further insight into the state of the noble metals present in the flame-derived catalysts. As regards the spectra intensities, similar signal intensity for comparable materials were observed with the exception of the Pt-only catalysts showing a three times lower signal intensity. The higher intensity of the vibrational bands observed with Rh-only catalysts reflects the higher amount of CO chemisorbed. For chemisorbed CO on Rh, three vibrational modes have been identified: dicarbonyl species at 2104 cm^{-1}, linear-bonded CO at around 2034 cm^{-1} and bridged CO at 1870 cm^{-1} [39]. In Fig. 4 all signals have their maximum below 2100 cm^{-1} and therefore the presence of dicarbonyl adsorption on Rh can be neglected, typically assigned to extremely small Rh clusters (<1 nm) or atomically dispersed Rh^{1+} sites [47]. Linear and bridged CO can be associated with CO adsorption on crystalline Rh sites [39]. Similar assignments have been found also for CO–Pt bonding [48]. The DRIFT spectra in Fig. 4 show the typical linear CO bonding at around 2080 cm^{-1} and a broad band at 1800 cm^{-1} assigned to bridged CO. From the areas below linear and bridged CO, the average stoichiometric factors (SFs) were calculated (Table 1).

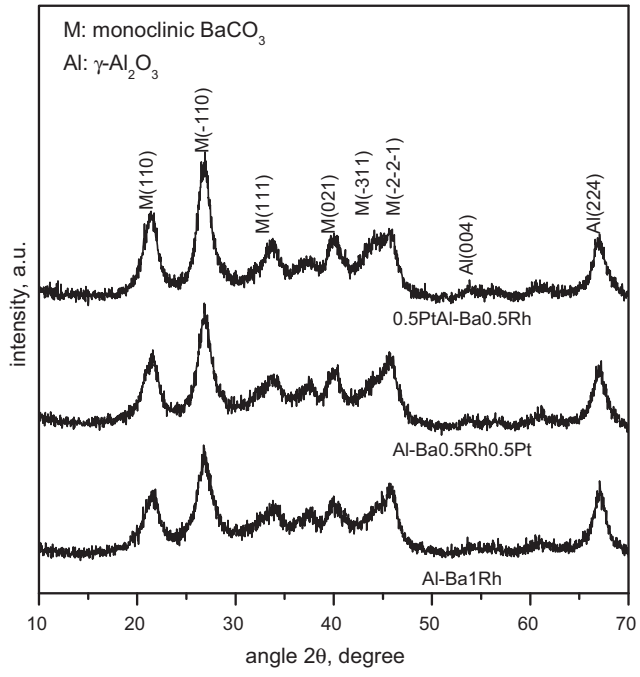

Fig. 3. XRD patterns of selected as-prepared catalysts. Characteristic reflections of monoclinic $BaCO_3$ (ICSD: 63257) and Al_2O_3 (ICSD: 99836) are indicated.

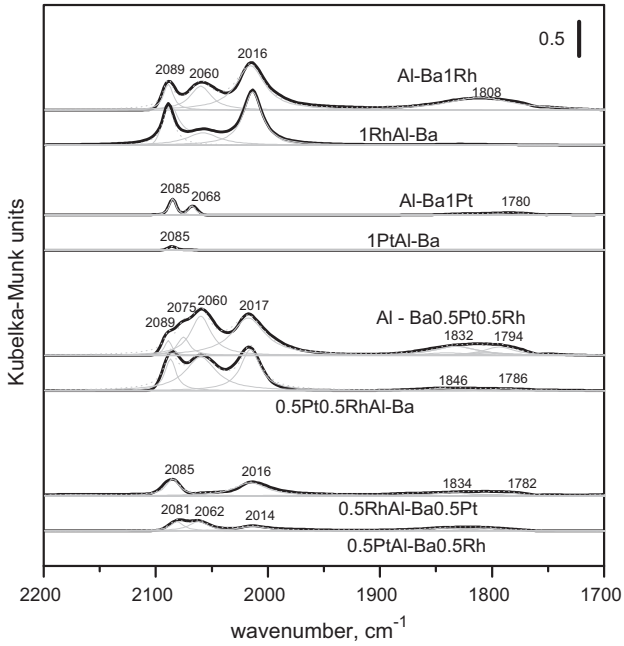

Fig. 4. DRIFT spectra of CO adsorption and the deconvoluted components of the CO bands for Rh and/or Pt deposited on Al_2O_3 or $BaCO_3$. The deconvoluted components are represented with dashed and gray lines, respectively.

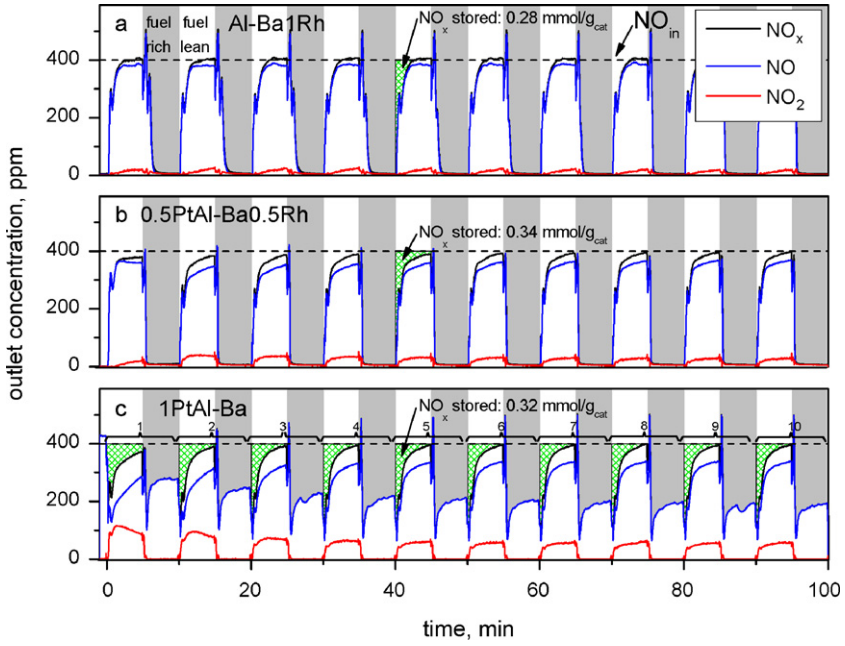

Fig. 5. Reactor outlet concentrations of NO_x (NO, NO_2) without sulfur dosing for selected catalysts: (a) Al-Ba1Rh (b) 0.5PtAl-Ba0.5Rh and (c) 1PtAl-Ba. While (a) and (b) stored NO_x under fuel lean conditions, (c) PtAl-Ba had difficulties to reduce NO_x under fuel rich conditions. The cycles are numbered 1–10 and the fuel lean/rich periods are illustrated in (a). The stored NO_x equivalent area is highlighted. Conditions: fuel lean period: 400 ppm NO, 500 ppm C_3H_6, and 8% O_2, balance He. Fuel rich period: 400 ppm NO and 500 ppm C_3H_6, balance He. Both at 300 °C and space velocity of 300,000 h^{-1}.

Basic surfaces increase the ratio of bridged to linear bonded CO [49] caused by the increase of the electron density of the noble metal [50]. Therefore noble metals deposited on $BaCO_3$ had higher SFs than those on Al_2O_3. This trend can be seen in Table 1 for: Rh-only (1RhAl-Ba, SF = 1.01 < Al-Ba1Rh, SF = 1.17), Pt-only (1PtAl-Ba, SF = 1.16 < Al-Ba1Pt, SF = 1.30) and even for the *mixed* Rh/Pt catalysts (0.5Rh0.5PtAl-Ba, SF = 1.04 < Al-Ba0.5Pt0.5Rh, SF = 1.13). For *separated* Rh and Pt both SFs were in the same order (1.25 and 1.22).

As will be shown later in Section 3.2, the metal dispersion alone was not the main factor determining the catalysts' activity. The location of noble metal on the catalysts was found to be even more crucial for efficient NO oxidation and reduction.

3.2. Catalytic behavior

The catalytic tests aimed at elucidating the influence of the controlled deposition of the noble metals (Pt, Rh) on the storage and support constituents on the NSR performance of the flame-made catalysts. For this purpose the catalytic behavior was investigated in the absence and presence of SO_2 in the feed.

3.2.1. Sulfur-free NO_x storage and reduction

In Fig. 5 the outlet NO_x concentrations for three selected catalysts[1] are compared during the first ten sulfur-free cycles. At the positions where conditions are changed from lean to rich cycles, a NO_x breakthrough peak appeared in all cycling experiments. The intensity of this breakthrough peak depended on the catalyst type. The small spikes observed at the change from reach to lean conditions are due to an apparative artifact caused by the switching as blind tests revealed.

Among the three catalysts shown in Fig. 5, 0.5PtAl-Ba0.5Rh (Fig. 5b) showed the highest NO_x storage capacity (0.34 mmol/g) and overall NSR performance followed by 1PtAl-Ba (Fig. 5c) (0.32 mmol/g) and Al-Ba1Rh (0.28 mmol/g (Fig. 5a). Note that the storage material was regenerated to the same level after each cycle, showing constant storage capacity. The storage capacity did not significantly vary depending on the noble metal or its preferential deposition, as the Ba-loading was the same for all catalysts investigated and the storage time was chosen long enough to reach an uptake close to saturation as will be shown later in Fig. 6. While during the lean cycle virtually no NO_2 was observed with Al-Ba1Rh, and only little with 0.5PtAl-Ba0.5Rh, 1PtAl-Ba showed significant amount of NO_2. The behavior is attributed to the high NO oxidation activity of Pt combined with a less efficient regeneration of the storage component ($BaCO_3$) during the rich phase. Similar behavior was observed for $Pt/Ba/Al_2O_3$ and $Pt\text{-}Rh/Ba/Al_2O_3$ catalysts by Amberntsson et al. [21], although the NO_x concentration was lower (100 ppm) and experiments were performed at higher temperature (400 °C) and lower space velocity (38,000 h^{-1}).

In order to gain further information on the storage and reduction behavior, the best catalyst of this series (0.5PtAl-Ba0.5Rh) was exposed to 1 h lean and 1 h rich cycles (Fig. 6b). Complete NO_x saturation was observed after about 20 min (Fig. 6a). The NO_x uptake rate decreased with time, as saturation was approached. Fast uptake in the beginning is attributed to formation of surface nitrates, while in a later stage NO_x has to diffuse into the bulk of the storage component [51]. During the fuel rich phase in Fig. 6b all NO_x is reduced during the first minutes, however, NO_x concentration increases with time probably due to a reversible self poisoning of the noble metal [53] with oxygen from the NO [52]. The substantial outlet concentration of NO_x during the rich period is a consequence of the very high space velocity used. From Fig. 6 it can be concluded that the choice of much shorter lean-rich cycling periods would probably be advantageous when using such a high space velocity. Proper adjustment of both cycling periods as well as space velocity is essential for optimal catalyst performance.

3.2.2. NO_x storage and reduction in the presence of SO_2

After the first ten sulfur-free cycles (Fig. 5), 25 ppm SO_2 was dosed to the inlet gas (5 min fuel lean and 5 min fuel rich conditions). Fig. 7 shows the NO_x outlet concentration for selected

[1] Later on we will show that the bimetallic 0.5PtAl-Ba0.5Rh is the best among the tested catalyst, therefore it is here compared to the monometallic Al-Ba1Rh and 1PtAl-Ba.

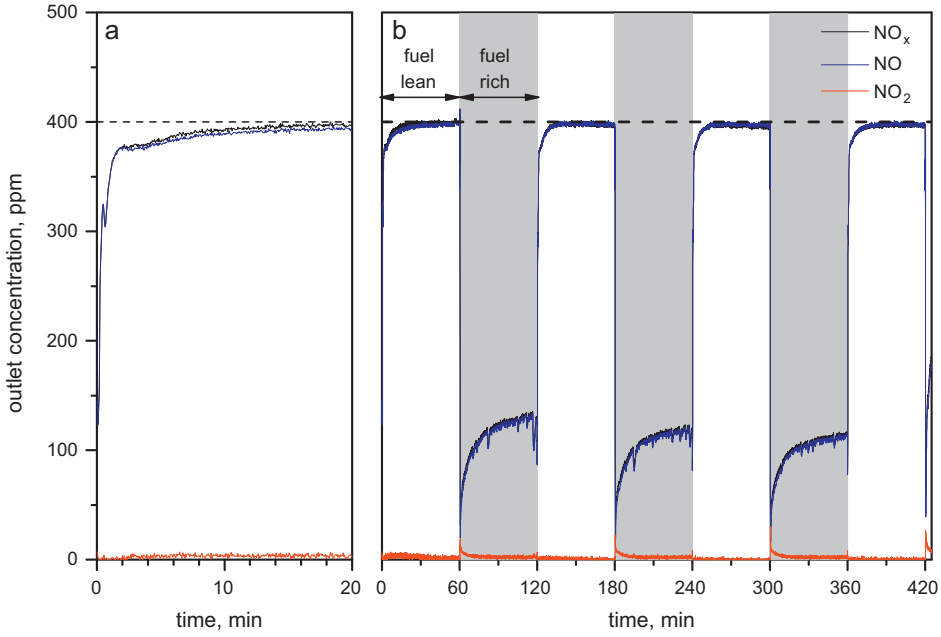

Fig. 6. Complete storage and reduction of 0.5PtAl-Ba0.5Rh catalysts in the absence of SO_2. (a) First 20 min of fuel lean cycle, (b) first 4 cycles. Conditions: fuel lean period: 400 ppm NO, 500 ppm C_3H_6, and 8% O_2, balance He. Fuel rich period: 400 ppm NO and 500 ppm C_3H_6, balance He. Both at 300 °C and space velocity of 300,000 h^{-1}.

catalysts. For Al-Ba1Rh (Fig. 7a) the first fuel lean/rich cycle was not affected by the presence of SO_2, and almost no NO_x was emitted during the fuel rich phase. During the second and third cycle, the NO_x emission during the fuel rich conditions increased, becoming constant at about 60 ppm (Fig. 7a). During fuel rich conditions, NO_x, from the engine off-gas, can be converted directly according to the three-way catalyst principle. Furthermore the saturated storage sites (here $Ba(NO_3)_2$) must be regenerated (to $BaCO_3$ or BaO) to store NO_x during the subsequent fuel lean cycle. If the Ba component is not regenerated properly, the storage capacity is lost very quickly as observed for Al-Ba1Pt, where after addition of 25 ppm SO_2 almost no NO_x (0.07 mmol/g_{cat}, Fig. 7d) is stored anymore. Note that in Fig. 7d the NO_x concentration during the fuel rich condition is higher than the actual 400 ppm NO_x inlet concentration, which is an artifact caused by the analytical system (CLD), where the gas is sampled based on pressure difference through a critical orifice. The indicated NO_x signal during the fuel rich condition is therefore higher than the actual NO_x concentration. Note that the underestimation of the NO_x conversion was maximal 5%. The NO_x reduction activity during the fuel rich cycle is very important for sustaining the overall NSR performance. When the regeneration (reduction/decomposition) of the stored NO_x is insufficient less NO_x can be stored during the subsequent fuel lean cycle. The NO_x storage capacity increased from 0.28 mmol/gcat (Fig. 5a) to 0.33 mmol/gcat

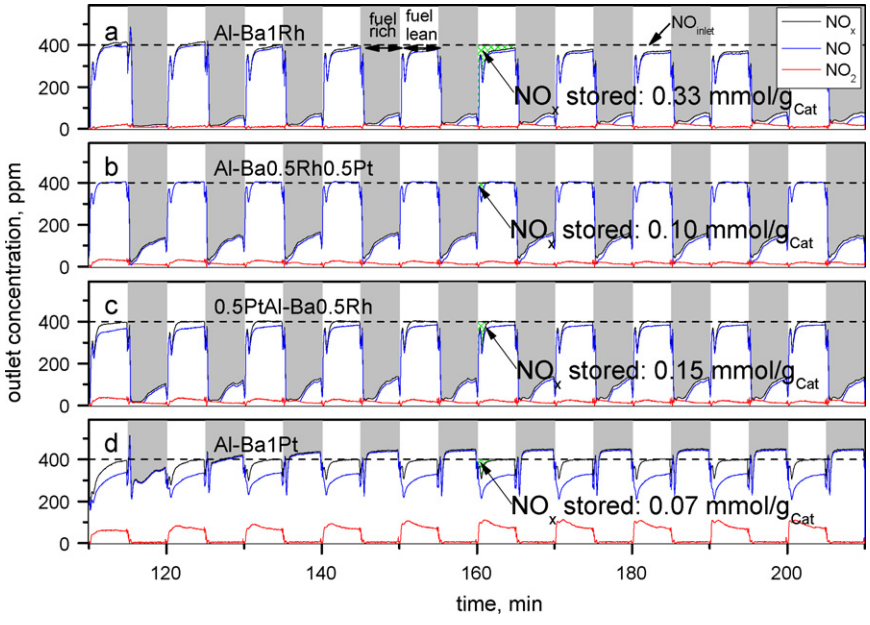

Fig. 7. Reactor outlet concentration of NO_x (NO, NO_2) with 25 ppm SO_2 dosing for selected catalysts: (a) Al-Ba1Rh, (b) Al-Ba0.5Rh0.5Pt, (c) 0.5PtAl-Ba0.5Rh, and (d) Al-Ba1Pt. SO_2 reduced the storage capacity of all catalysts and the NO_x reduction efficiency during fuel rich conditions. Conditions: fuel lean period: 400 ppm NO, 500 ppm C_3H_6, 25 ppm SO_2, and 8% O_2, balance He. Fuel rich period: 400 ppm NO and 500 ppm C_3H_6, 25 ppm SO_2, balance He. Both at 300 °C and space velocity of 300,000 h^{-1}.

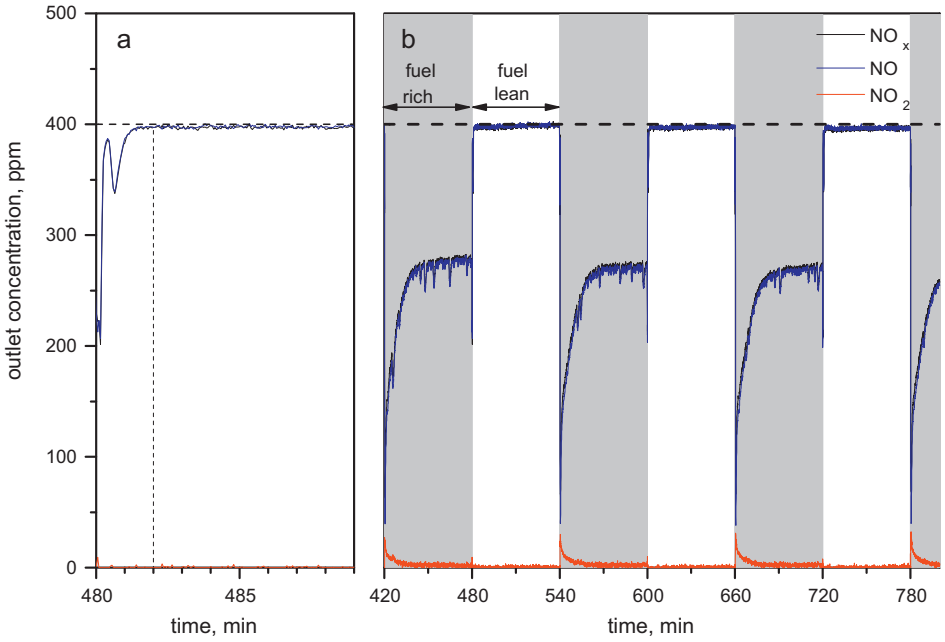

Fig. 8. Complete storage and reduction of 0.5PtAl-Ba0.5Rh catalysts in the presence of 25 ppm SO_2. (a) First 10 min of fuel lean cycle and (b) complete 3 cycles. Conditions: fuel lean period: 400 ppm NO, 500 ppm C_3H_6, 25 ppm SO_2, and 8% O_2, balance He. Fuel rich period: 400 ppm NO and 500 ppm C_3H_6, 25 ppm SO_2, balance He. Both at 300 °C and space velocity of 300,000 h^{-1}.

in the presence of SO_2. Such an increase of about 20% of the NO_x storage capacity was already observed for SO_2 exposure during the fuel rich phase [20], although only for one cycle. This effect was explained by the reduction of platinum oxides to metallic platinum by SO_2 [14]. This favors the NO to NO2 oxidation which enhances NO_x storage [20].

The *mixed* Rh/Pt on $BaCO_3$ (Al-Ba0.5Rh0.5Pt, Fig. 7b) also deactivated in the presence of SO_2. During the fuel rich phase, considerable amount of NO_x was detected in the reactor outlet stream. The NO_x reduction activity was reduced and 150 ppm of NO_x outlet concentration was measured, 2.5 times higher than that for the Rh-only catalyst (Fig. 7a). For Al-Ba0.5Rh0.5Pt the NO_x storage ability decreased to 0.10 mmol/g and the NO_x outlet reached the NO_{inlet} level after the first minute. Compared to the *mixed* Rh/Pt, the *separated* Rh-Pt (0.5PtAl-Ba0.5Rh, Fig. 7c) showed a better performance, although the materials' composition was the same. During fuel rich conditions, not all inlet NO was reduced and an outlet concentration of 110 ppm NO_x was measured, which was twice that observed with the Rh-only catalyst (Fig. 7a). This can be explained by the contribution of Rh in these catalysts, as for NO_x reduction Pt deactivates in the presence of SO_2 [21]. The storage capacity was 0.15 mmol/g (Fig. 7c) corresponding to about 45% of that achieved in experiments without addition of 25 ppm SO_2 (Fig. 5b) and more NO_2 was produced compared to Rh-only catalysts

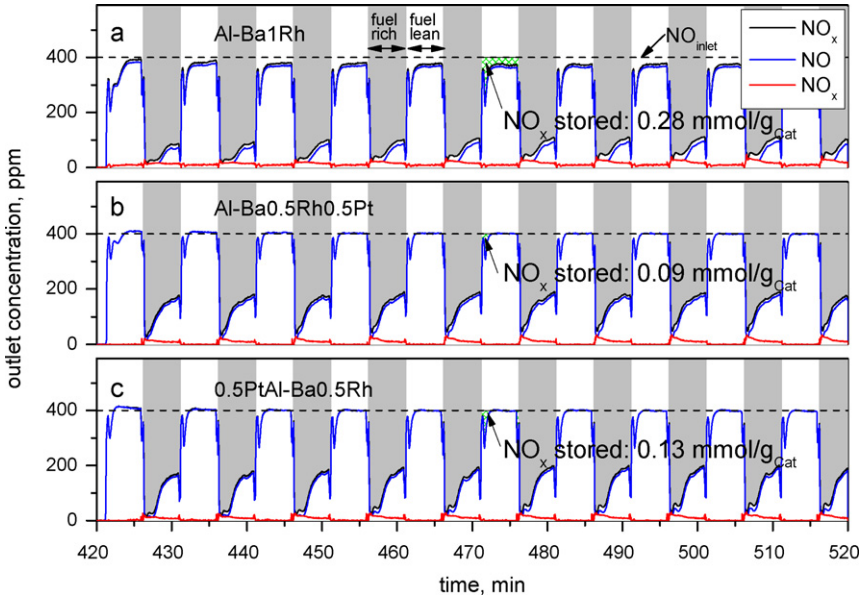

Fig. 9. Reactor outlet concentration of NO_x (NO, NO_2) with 25 ppm SO_2 after desulfation for selected catalysts: (a) Al-Ba1Rh, (b) Al-Ba0.5Rh0.5Pt, and (c) 0.5PtAl-Ba0.5Rh. The desulfation process did not significantly alter the catalyst performance after the second cycle. Conditions: fuel lean period: 400 ppm NO, 500 ppm C_3H_6, 25 ppm SO_2, and 8% O_2, balance He. Fuel rich period: 400 ppm NO and 500 ppm C_3H_6, 25 ppm SO_2, balance He. Both at 300 °C and space velocity of 300,000 h^{-1}.

(Fig. 7a). A similar effect of Rh was reported by Amberntsson et al. [21], where Pt had a higher NO to NO_2 oxidation activity in the presence of SO_2 than Rh-containing NSR catalysts. As NO_2 is typically stored faster on $BaCO_3$ [54], the effluent NO_2 is an indication that not enough storage sites ($BaCO_3$) were available. Increasing the Ba loading or the $BaCO_3$ surface could improve NO_x storage [55].

Fig. 8a shows full storage of NO_x in the presence of SO_2, after the *separated* Rh-Pt catalyst was cycled three times (60 min fuel lean and 60 min fuel rich) with NO_x and SO_2 (Fig. 8b). The storage capacity clearly was reduced with SO_2 dosed over time.

3.2.3. NO_x storage and reduction in the presence of SO_2 after regeneration

Fig. 9 shows the NO_x outlet concentration *in the presence of* SO_2 after catalysts were desulfated. At elevated temperature the catalyst performance typically decreases as for noble metal sintering and catalyst aging [56]. When comparing the performance before (Fig. 7) and after desulfation (Fig. 9), it becomes evident that the Al-Ba1Rh can be regenerated from sulfur poisoning (for the first cycle), enabling also the evaluation of its stability e.g. if the preferential location was kept or was lost by the sintering process.

The Pt-only catalysts (Al-Ba1Pt (Fig. 7d) and 1PtAl-Ba), that lost their performance in the presence of 25 ppm SO_2, did not recover to the initial storage capacity (Fig. 10b), only when the catalyst was tested without SO_2 after desulfation (Fig. 10b, series 4) some of the initial NO_x conversion was recovered. It was therefore not so much the catalysts' thermal aging but the SO_2 poisoning of Pt that limited the performance of these catalysts. Desulfation had a positive effect in the first cycle (Fig. 9), almost all catalysts showed a higher NO_x conversion in the first cycle after desulfation (series 3) compared prior to desulfation (series 2). During the fuel rich period the content of unreduced NO_x was the lowest for the Al-Ba1Rh catalyst (100 ppm, Fig. 9a), it increased for *separated* Rh on $BaCO_3$ and *mixed* Rh/Pt on $BaCO_3$ (180 ppm, Fig. 9b) and Pt on Al_2O_3 (160 ppm, Fig. 9c). The highest NO_x reduction activity for Al-Ba1Rh is attributed to the higher Rh loading. The bimetallic Rh-Pt catalysts had the same Rh loading but the *separated* Rh and Pt had a slightly higher conversion (NO_x reduction activity) that could be explained by a higher surface area (Al_2O_3 and $BaCO_3$) and higher dispersion (see Table 1), resulting in lower noble metal concentration per surface area making *separated* Rh and Pt less likely to sinter [31] and therefore able to retain a higher NO_x reduction activity. CO chemisorption measurements after similar heat treatment at 750 °C but without exposure of the catalysts to SO_2 showed a reduced dispersion for catalysts where the noble metal(s) was only deposited on one component, as in Al-Ba1Pt and Al-Ba0.5Rh0.5Pt, where the dispersion (cf. Table 1) decreased to 5.5 and 3.7%, respectively. In contrast, the dispersion of 0.5PtAl-Ba0.5Rh remained constant at 15%.

3.2.4. NO_x conversion of bimetallic catalysts with different Pt and Rh location

Fig. 10 summarizes the NO_x conversion of all catalysts as a function of cycle number: (1) cycle 1–10, NO_x conversion without SO_2 exposure, (2) cycle 11–20 NO_x conversion in the presence of 25 ppm SO_2. After 20 cycles the catalyst was desulfated at 750 °C and cooled down to 300 °C and subsequently exposed to cycling with 25 ppm SO_2 in the feed (3) cycles 21–30). Note that the inlet conditions of the second and third stages were the same.

Fig. 10a shows that the catalyst with Rh on $BaCO_3$ (Ba) (circles, Al-Ba1Rh) performed better than the one with Rh on Al_2O_3 (Al) (triangles, 1RhAl-Ba) in all test series 1–3. Both catalysts showed an increase of the NO_x conversion, more pronounced with 1RhAl-Ba, with cycle number in the SO_2-free cycles. Catalyst storage and reduction improved during the first cycles, similar to as-prepared $Pt/Ba/Al_2O_3$ catalysts (without reduction before catalytic testing) [36]. In the presence of SO_2 (test series 2, cycles 11–20), the NO_x conversion first slightly decreased before increasing again (Fig. 10a), indicating that partial poisoning of the noble metal can be beneficial for NO oxidation rate [11]. SO_2 had a stronger influence on the NSR behavior of 1RhAl-Ba but the catalyst regained its performance after 10 cycles (Fig. 10a). After desulfation at 750 °C, there was little difference between both Rh-only catalysts because at high temperature the advantage of preferential deposition of noble metals was lost similarly as previously observed for $Pt/K_2CO_3/Al_2O_3$ catalysts [57]. This indicates a significant improvement for the 1RhAl-Ba catalysts and a slight loss of activity for Al-Ba1Rh.

Compared to Rh, Pt-only NSR catalysts showed completely different behavior (Fig. 10b). In the absence of SO_2 (series 1), for Pt on Al_2O_3 (1PtAl-Ba, triangles) a higher NO_x conversion was observed, as Al-Pt is a highly active catalyst for NO oxidation [34] and NO_2 is stored rapidly on the $BaCO_3$ [54]. With prolonged cycling, Al-Ba1Pt (circles) increased its performance as NO_x reduction during the fuel rich period became the limiting step for the overall NSR performance instead of NO oxidation during the fuel lean period. In the presence of SO_2, however, both catalysts lost their NO_x conversion activity completely with increasing cycle number. As seen in Fig. 7d, the Pt-only catalysts neither stored nor reduced NO_x efficiently in the presence of SO_2. This is in agreement with Amberntsson et al. [21] confirming that Pt is not able to regenerate the catalytic system and therefore NO_x cannot be stored. Also desulfation of the Pt catalysts (Fig. 10b, series 3) did not increase the NO_x conversion as the Pt sites were poisoned immediately. Catalytic tests after desulfation without SO_2 in the feed (Fig. 10b, series 4) showed that the catalyst only regained part of its NSR activity, which is attributed to some sintering and/or restructuring during the high temperature desulfation.

When combining both Rh and Pt (Fig. 10c), lower NO_x conversion was measured compared to the Rh- and Pt-only catalysts (Fig. 10a and b). When Rh and Pt were deposited on $BaCO_3$ (Al-Ba0.5Rh0.5Pt), the NO_x conversion was about 40% (circles, Fig. 10c) and decreased to about 30% in the presence of SO_2. This decrease originates from the loss of NO_x reduction efficiency during the fuel rich phase (because SO_2 poisons the noble metal) decreasing also the storage capacity (compare Fig. 7b). Also desulfation had relatively little influence on the catalyst performance (cycles 21–30), showing that the catalyst did not deteriorate at the conditions applied. For Rh and Pt on Al_2O_3 (triangles, 0.5Rh0.5PtAl-Ba), the catalyst performance was unsteady and inferior to that of Rh/Pt on $BaCO_3$.

Separated Rh and Pt presented in Fig. 10d showed the best performance with Pt on Al_2O_3 and Rh on $BaCO_3$ (circles, 0.5PtAl-Ba0.5Rh). This was expected, as NO oxidation on Pt is not limited in the presence of SO_2 while Rh is sulfur-tolerant for NO_x reduction during fuel rich conditions [21]. Under SO_2-free conditions, this catalyst showed the best performance while in the presence of SO_2, NO_x conversion decreased from 53% to 42% as the reduction activity was partially lost during fuel rich conditions (see Fig. 7c) and the storage capacity on $BaCO_3$ was lost too (see Figs. 6b and 8b). After desulfation NO_x conversion decreased to 37% and was therefore slightly lower than for Rh-only catalysts (44%, Fig. 10a). Although it should be reminded that the *separated* Rh/Pt catalysts contained only half of the amount of Rh compared to the Rh-only catalyst (but constant weight loading of noble metals).

The catalytic studies on the flame-made mono- and bimetallic NSR catalysts prepared by controlled deposition of the noble metals on storage and support confirmed that combinations of Rh and Pt can be attractive, as Pt alone did not reduce NO_x in the presence of SO_2 (Fig. 10b). Rh/Pt mixtures might be considered e.g. when the price of Rh is not extremely high. In 2008 the Rh price had risen

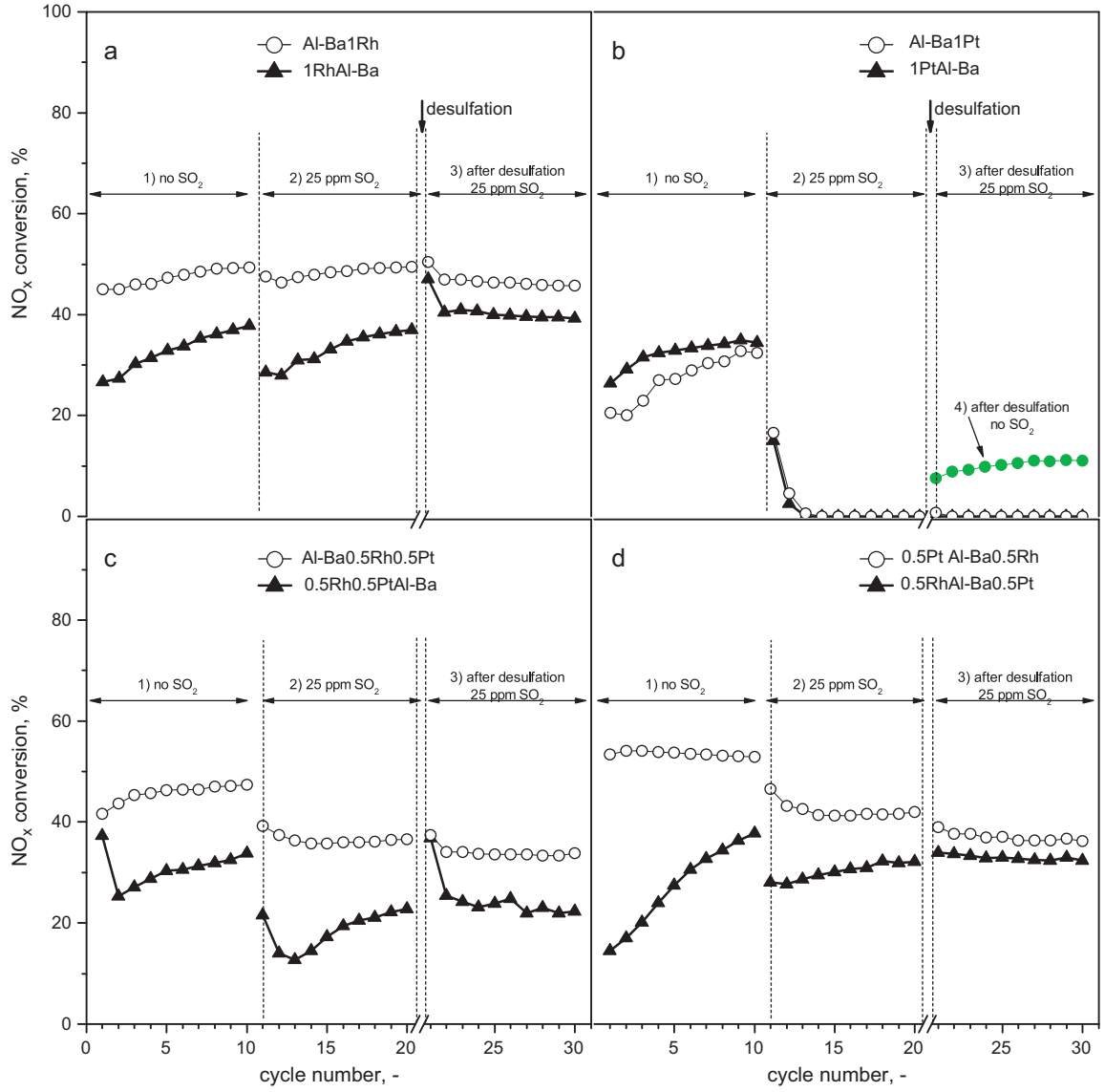

Fig. 10. NO_x conversion of catalysts during cycling under different conditions at 300 °C: (series 1) in absence of SO_2; (series 2) in presence of SO_2; (series 3) in presence of SO_2 after desulfation with 2%H_2 at 750 °C. Monometallic catalysts (a) Rh-only, (b) Pt-only; bimetallic catalysts, (c) *mixed* Rh/Pt, and (d) *separated* Rh-Pt. In (b) a catalyst was tested without SO_2 after the desulfation (series 4).

up to 10,000 US$/oz,[2] while the current price (2010) for Rh is 2500 US$/oz, still 47% higher than that of Pt (in 2010 the highest price was 1700 US$/oz) [58].

Clearly our study indicates that the performance of mono- and bimetallic Rh and Pt catalysts can considerably be improved when noble metals are deposited optimally e.g. Pt on the Al_2O_3 support and Rh on the $BaCO_3$ storage component. In contrast, lower activity is obtained when Pt and Rh are deposited reversely (Fig. 10d, triangles). In bimetallic catalysts, that is in combinations of Pt with Rh, the sulfur tolerance was always guaranteed, while complete deactivation was observed when Pt-only catalysts were used (Fig. 10b).

Considering the NSR performance and the metal dispersions determined for the different catalysts (Table 1), no direct correlation is evident, for example Pt-only catalysts exhibited a high dispersion, above 30%, while Rh-only catalysts showed a much lower dispersion but high NO_x conversion (Fig. 10a). For combined Rh/Pt, the catalysts with higher dispersion showed lower NO_x conversion in the presence of sulfur, indicating that the effect of the noble metal location had a more prominent effect on the NSR performance than the noble metal dispersion.

3.2.5. NO_x conversion at different space velocity

In order to gain some insight about the behavior of some selected catalysts at lower space velocity (SV), similar series of experiments were performed at SV of 38,000 h^{-1}. In Fig. 11a) the performances of two representative catalysts (0.5PtAl-Ba0.5Rh and Al-Ba1Pt) at SV = 38,000 h^{-1} (open symbols) and SV = 300,000 h^{-1} (filled symbols) are compared. As expected, at lower SV, the NO_x conversion was higher and the time to reach steady state was longer, especially for the series of experiments where SO_2 was present in the feed. While at SV = 300,000 h^{-1} steady-state in NO_x conversion was reached with 0.5PtAl-Ba0.5Rh after 3 cycles at SV = 38,000 h^{-1}, in the presence of SO_2. NO_x conversion observed with both catalysts still decreased even after 20 cycles. After desulfation (series 3 in Fig. 11) the observation made in Fig. 10 that Rh is more resistant toward SO_2 poisoning is corroborated also by the experiments

[2] oz = troy ounce: unit of weight used in noble metal trading. 1 troy ounce ≈ 31.1 g.

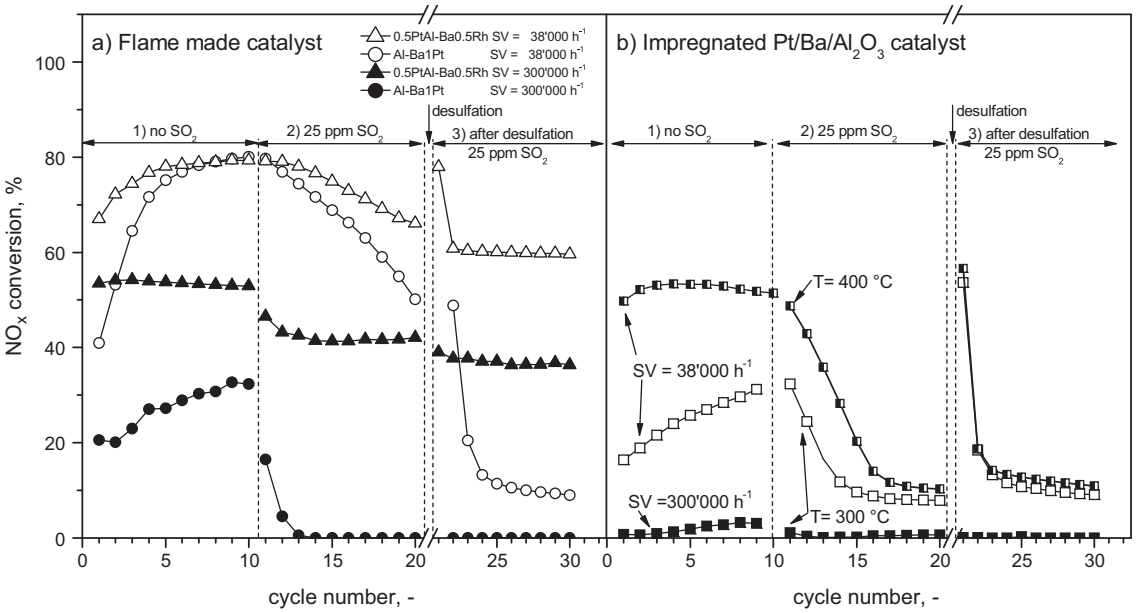

Fig. 11. NO_x conversion of selected flame-made catalysts, Al-Ba1Pt and 0.5PtAl-Ba0.5Rh, and impregnated $Pt/Ba/Al_2O_3$ reference catalyst during cycling at different space velocities, 38,000 h^{-1} (open symbols) and 300,000 h^{-1} (full symbols) Ia) flame made catalysts Al-Ba1Pt (circle) and 0.5PtAl-Ba0.5Rh (triangles) are compared. In b) the catalytic performance of the wet-impregnated $Pt/Ba/Al_2O_3$ reference catalyst (squares) at the same testing conditions is shown at 300 °C and at 400 °C.

performed at 38,000 h^{-1}. The impregnated $Pt/Ba/Al_2O_3$ reference catalyst (Fig. 11b) shows similar conversion trends like the flame made catalyst under the different conditions (1–3), albeit at much lower NO_x conversion. At high SV = 300,000 h^{-1} almost no NO_x was converted while at 38,000 h^{-1} a similar performance like the flame made catalysts at 300,000 h^{-1} was observed (compare Fig. 11a and b). Testing the impregnated catalysts at 400 °C resulted in a performance comparable to literature [20], proving the reliability of the testing procedure and the superior performance of the flame made catalysts Al-Ba1Pt compared to the classical wet-impregnated reference catalyst. The main difference between the these catalysts is the preferential deposition of the Pt in the flame-made catalyst and the fact that this catalyst is only exposed very shortly to high temperatures in the preparation process while the impregnation catalyst needs annealing at elevated temperatures (500 °C) for several hours (5 h) [38]. Interestingly, the superior activity was largely lost after the desulfation at 750 °C (series 3 in Fig. 11a,b) where both the flame-derived and the impregnated $Pt/Ba/Al_2O_3$ catalysts showed similar NO_x conversion at SV = 38,000 h^{-1}.

Finally, it should be mentioned that the differences in the catalytic behavior observed for the various catalysts investigated in this study may vary depending on the experimental conditions, such as temperature, type of reductant, duration of lean/reach periods, and space velocity, which in a catalyst bed may lead to different time-dependent chemical and structural gradients [59,60]. Nevertheless, these factors will hardly bias our general conclusion that the preferential deposition of the noble metals either on the storage or support component of mono- and bimetallic catalysts will allow to improve the performance of NSR catalysts.

4. Conclusions

Mono- and bimetallic rhodium and platinum containing NSR catalysts were prepared using a twin nozzle FSP setup allowing preferential deposition of the noble metals on support (Al_2O_3) and storage component ($BaCO_3$). All catalysts were tested in the presence and absence of SO_2. CO adsorption combined with DRIFTS revealed significant differences in the vibrational bands depending on the noble metal and its supporting constituent (Al_2O_3 or $BaCO_3$). While the type of noble metal and the location of its deposition had a strong influence on the NSR efficiency, the effect of the noble metal dispersion was less prominent. Rhodium containing catalysts showed higher NO_x conversion as well as a higher resistance toward SO_2 poisoning and relatively little loss of activity upon thermal aging at 750 °C. Combinations of Rh and Pt showed good NO_x reduction efficiency especially when Rh was located on $BaCO_3$. Best NSR performance was observed with bimetallic catalysts where the noble metals were separated, that is with Pt on Al_2O_3 and Rh on $BaCO_3$.

Acknowledgements

We thank Dr. Frank Krumeich (ETH) for STEM/EDXS investigation and the Electron Microscopy Center of ETH Zurich (EMEZ) for providing the necessary infrastructure. We greatly appreciated the financial support by ETH Zürich (TH-09 06-2) and the European Research Council/European Community (under FP7). We thank for the contribution of platinum chemicals by Johnson Matthey PLC.

References

[1] P. Granger, V.I. Parvulescu, Chem. Rev. 111 (2011) 3155–3207.
[2] M.D. Amiridis, T.J. Zhang, R.J. Farrauto, Appl. Catal. B: Environ. 10 (1996) 203–227.
[3] N. Miyoshi, S. Matsumoto, K. Katoh, T. Tanaka, J. Harada, N. Takahashi, K. Yokota, M. Sugiura, K. Kasahara, SAE Technical Paper 950809, 1995.
[4] S. Roy, A. Baiker, Chem. Rev. 109 (2009) 4054–4091.
[5] J.E. Kirwan, M. Shost, G. Roth, J. Zizelman, SAE Technical Paper 2010-01-0590, 2010.
[6] R. Strobel, F. Krumeich, S.E. Pratsinis, A. Baiker, J. Catal. 243 (2006) 229–238.
[7] M. Casapu, J.D. Grunwaldt, M. Maciejewski, A. Baiker, M. Wittrock, U. Gobel, S. Eckhoff, Top. Catal. 42-43 (2007) 3–7.
[8] S. Matsumoto, Y. Ikeda, H. Suzuki, M. Ogai, N. Miyoshi, Appl. Catal. B: Environ. 25 (2000) 115–124.
[9] S.Q.A. Rizvi, Lubric. Eng. 55 (1999) 33–39.
[10] N. Takahashi, A. Suda, I. Hachisuka, M. Sugiura, H. Sobukawa, H. Shinjoh, Appl. Catal. B: Environ. 72 (2007) 187–195.
[11] A. Amberntsson, M. Skoglundh, M. Jonsson, E. Fridell, Catal. Today 73 (2002) 279–286.
[12] E. Fridell, H. Persson, L. Olsson, B. Westerberg, A. Amberntsson, M. Skoglundh, Top. Catal. 16 (2001) 133–137.
[13] H.C. Yao, H.K. Stepien, H.S. Gandhi, J. Catal. 67 (1981) 231–236.

[14] A.F. Lee, K. Wilson, R.M. Lambert, C.P. Hubbard, R.G. Hurley, R.W. McCabe, H.S. Gandhi, J. Catal. 184 (1999) 491–498.
[15] M.A. Newton, A.J. Dent, S. Diaz-Moreno, S.G. Fiddy, B. Jyoti, J. Evans, Chem. Commun. (2003) 1906–1907.
[16] M. Bowker, Chem. Soc. Rev. 37 (2008) 2204–2211.
[17] V. Schmeisser, J.D. Perez, U. Tuttlies, G. Eigenberger, Top. Catal. 42-43 (2007) 15–19.
[18] N.S. Nasri, J.M. Jones, V.A. Dupont, A. Williams, Energy Fuels 12 (1998) 1130–1134.
[19] J.S. Hepburn, H.G. Stenger, Energy Fuels 2 (1988) 289–292.
[20] A. Amberntsson, M. Skoglundh, S. Ljungstrom, E. Fridell, J. Catal. 217 (2003) 253–263.
[21] A. Amberntsson, E. Fridell, M. Skoglundh, Appl. Catal. B: Environ. 46 (2003) 429–439.
[22] M.J. Patterson, D.E. Angove, N.W. Cant, Appl. Catal. B: Environ. 35 (2001) 53–58.
[23] J. Jelic, R.J. Meyer, Catal. Today 136 (2008) 76–83.
[24] W.S. Epling, L.E. Campbell, A. Yezerets, N.W. Currier, J.E. Parks, Catal. Rev. Sci. Eng. 46 (2004) 163–245.
[25] P. Engstrom, A. Amberntsson, M. Skoglundh, E. Fridell, G. Smedler, Appl. Catal. B: Environ. 22 (1999) L241–L248.
[26] R. Strobel, A. Baiker, S.E. Pratsinis, Adv. Powder Technol. 17 (2006) 457–480.
[27] R. Strobel, L. Madler, M. Piacentini, M. Maciejewski, A. Baiker, S.E. Pratsinis, Chem. Mater. 18 (2006) 2532–2537.
[28] M. Piacentini, R. Strobel, M. Maciejewski, S.E. Pratsinis, A. Baiker, J. Catal. 243 (2006) 43–56.
[29] R. Büchel, R. Strobel, A. Baiker, S.E. Pratsinis, Top. Catal. 52 (2009) 1709–1712.
[30] R. Büchel, S.E. Pratsinis, A. Baiker, Appl. Catal. B: Environ. 101 (2011) 682–689.
[31] R. Strobel, J.D. Grunwaldt, A. Camenzind, S.E. Pratsinis, A. Baiker, Catal. Lett. 104 (2005) 9–16.
[32] P. Gelin, M. Primet, Appl. Catal. B: Environ. 39 (2002) 1–37.
[33] M. Yashima, L.K.L. Falk, A.E.C. Palmqvist, K. Holmberg, J. Colloid Interface Sci. 268 (2003) 348–356.
[34] B. Subramaniam, A. Varma, Chem. Eng. Commun. 20 (1983) 81–91.
[35] L. Olsson, E. Fridell, J. Catal. 210 (2002) 340–353.
[36] R. Büchel, R. Strobel, F. Krumeich, A. Baiker, S.E. Pratsinis, J. Catal. 261 (2009) 201–207.
[37] L. Madler, H.K. Kammler, R. Mueller, S.E. Pratsinis, J. Aerosol. Sci. 33 (2002) 369–389.
[38] M. Piacentini, M. Maciejewski, A. Baiker, Appl. Catal. B: Environ. 59 (2005) 187–195.
[39] J.T. Yates, T.M. Duncan, R.W. Vaughan, J. Chem. Phys. 71 (1979) 3908–3915.
[40] E. Schmidt, W. Kleist, F. Krumeich, T. Mallat, A. Baiker, Chem. Eur. J. 16 (2010) 2181–2192.
[41] N.S. Nesterenko, A.V. Avdey, A.Y. Ermilov, Int. J. Quantum Chem. 106 (2006) 2281–2289.
[42] A. Amberntsson, H. Persson, P. Engstrom, B. Kasemo, Appl. Catal. B: Environ. 31 (2001) 27–38.
[43] K.S. Kabin, R.L. Muncrief, M.P. Harold, Catal. Today 96 (2004) 79–89.
[44] E. Roedel, A. Urakawa, A. Baiker, Catal. Today 155 (2010) 172–176.
[45] R. Strobel, M. Maciejewski, S.E. Pratsinis, A. Baiker, Thermochim. Acta 445 (2006) 23–26.
[46] V. Ermini, E. Finocchio, S. Sechi, G. Busca, S. Rossini, Appl. Catal. A: Gen. 198 (2000) 67–79.
[47] M. Primet, J. Chem. Soc. Faraday Trans. 1 (74) (1978) 2570–2580.
[48] H. Tanaka, M. Kuriyama, Y. Ishida, S.I. Ito, T. Kubota, T. Miyao, S. Naito, K. Tomishige, K. Kunimori, Appl. Catal. A: Gen. 343 (2008) 125–133.
[49] F. Hoxha, B. Schimmoeller, Z. Cakl, A. Urakawa, T. Mallat, S.E. Pratsinis, A. Baiker, J. Catal. 271 (2010) 115–124.
[50] R.A. van Santen, J. Chem. Soc. Faraday Trans. 1 (83) (1987) 1915–1934.
[51] U. Tuttlies, V. Schmeisser, G. Eigenberger, Chem. Eng. Sci. 59 (2004) 4731–4738.
[52] R. Burch, T.C. Watling, Catal. Lett. 37 (1996) 51–55.
[53] R. Burch, P.J. Millington, A.P. Walker, Appl. Catal. B: Environ. 4 (1994) 65–94.
[54] M.O. Symalla, A. Drochner, H. Vogel, R. Büchel, S.E. Pratsinis, A. Baiker, Appl. Catal. B: Environ. 89 (2009) 41–48.
[55] M. Piacentini, M. Maciejewski, A. Baiker, Appl. Catal. B: Environ. 60 (2005) 265–275.
[56] M. Casapu, J.D. Grunwaldt, M. Maciejewski, A. Baiker, R. Hoyer, M. Wittrock, S. Eckhoff, Catal. Lett. 120 (2008) 1–7.
[57] R. Büchel, R. Strobel, A. Baiker, S.E. Pratsinis, Top. Catal. 52 (2009) 1799–1802.
[58] Johnson Matthey PLC, Platinum 2010 Interim Review, London, 2010.
[59] A. Urakawa, N. Maeda, A. Baiker, Angew. Chem. Int. Ed. 47 (2008) 9256–9259.
[60] N. Maeda, A. Urakawa, A. Baiker, J. Phys. Chem. C 113 (2009) 16724–16735.